7C.2

Entropy Ventilation in an Axisymmetric Tropical Cyclone Model

Brian H. Tang* and Kerry A. Emanuel
Massachusetts Institute of Technology, Cambridge, Massachusetts

1 Introduction

Ventilation of a tropical cyclone's inner core by low entropy environment air has been hypothesized to constrain tropical cyclone (TC) intensity (Simpson and Riehl 1958). The low entropy air is fluxed inward by asymmetries, such as vortex Rossby waves excited by environmental vertical wind shear. However, there is ambiguity as to the layer over which ventilation occurs and how ventilation precisely affects TC intensity. Frank and Ritchie (2001) hypothesized that the upper portion of the circulation is ventilated first, causing the TC to weaken from the top-down. On the other hand, Cram et al. (2007) found in their 3D numerical simulations of a sheared TC that the eyewall entropy is reduced by midlevel ventilation. The goals of this study are to assess the sensitivity of TC intensity to the location and amplitude of the ventilation and to study how ventilation induces axisymmetric weakening.

2 Model

The model used in this study is an nonhydrostatic, axisymmetric, and finite volume TC model. It is designed in the same spirit of simplicity as the the Rotunno and Emanuel (1987) model, but in contrast, uses a pseudoadiabatic-like entropy density as its thermodynamic variable and has much more rigorously conserved mass and entropy budgets. Ventilation is introduced by adding a term to the turbulent flux parameterization for entropy:

$$F_r^s = -A\mathcal{L}(r,z)\frac{\partial s}{\partial r}, \tag{1}$$

where A is the maximum amplitude of the viscosity, $\mathcal{L}(r,z)$ is a localization function that limits the areal extent of the ventilation, s is the moist entropy, and r is the radius. In the following experiments, the localization function is chosen such that F_r^s vanishes inside a radius of 20 km and outside a radius of 60 km and is limited to a 2 km vertical layer that is set *a priori*. Eddy momentum fluxes are ignored in this study in order to focus solely on the thermodynamic effect of ventilation.

Corresponding Author Address: Brian Tang, Massachusetts Institute of Technology, 77 Massachusetts Ave. #54-1721, Cambridge, MA 02139; E-mail: btangy@mit.edu

3 Sensitivity Experiments

The model is run at 2 km radial resolution and 0.3 km vertical resolution. A balanced, weak vortex is inserted into an neutrally stable environment with 28°C SST. The vortex takes about five to seven days to spin up to a steady-state intensity of 67-68 $\mathrm{m\ s^{-1}}$. After the TC reaches a steady-state for a reasonable period of time, the ventilation is turned on by applying (1). A suite of experiments, listed in Tab. 1, is used to assess the TC's sensitivity to the both the amplitude and height of the ventilation.

Table 1: Tropical cyclone ventilation experiments.

Experiment	Amplitude ($\mathrm{m^2\ s^{-1}}$)	Height (km)
Ctrl	0	NA
A01	1.0×10^4	3.0
A05	5.0×10^4	3.0
A10	1.0×10^5	3.0
A50/H03	5.0×10^5	3.0
H06	5.0×10^5	6.0
H09	5.0×10^5	9.0
H12	5.0×10^5	12.0
H15	5.0×10^5	15.0

a. *Amplitude*

In the first set of experiments, the amplitude of the eddy viscosity is varied from 1.0×10^4 $\mathrm{m^2\ s^{-1}}$ to 5.0×10^5 $\mathrm{m^2\ s^{-1}}$. The center of the mixing is placed at a radius of 30 km and height of 3 km, just radially outside the eyewall. Subsequently, diffusion of entropy down the radial gradient results in a decrease in the eyewall entropy and an increase in the near-inner core entropy between a height of 2-4 km.

The ventilation causes marked changes to the TC's structure in the first 12 hours, particularly for strong ventilation. Updrafts in the eyewall weaken as less buoyant parcels are entrained into it. In response to the weakening of the eyewall convective flux, the radial inflow and outflow also decrease in magnitude. Moreover, the outflow moves to a lower height as the eyewall buoyancy relative to the environment decreases. The upper-level warm core quickly weakens as well.

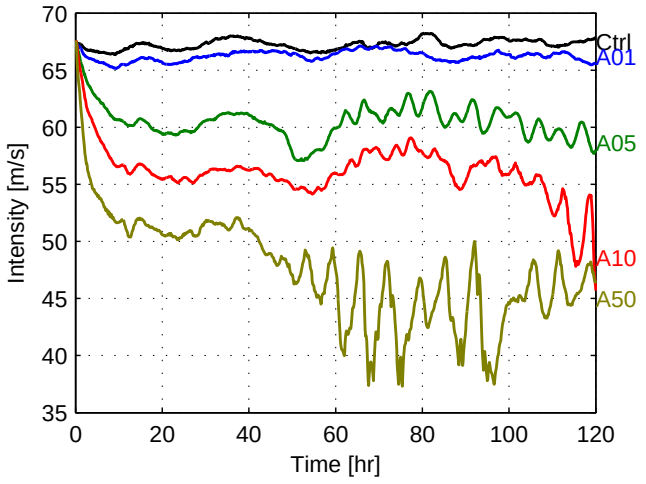

Figure 1: Maximum tangential winds ($\mathrm{m\ s^{-1}}$) in the 'A' ventilation experiments listed in Tab. 1.

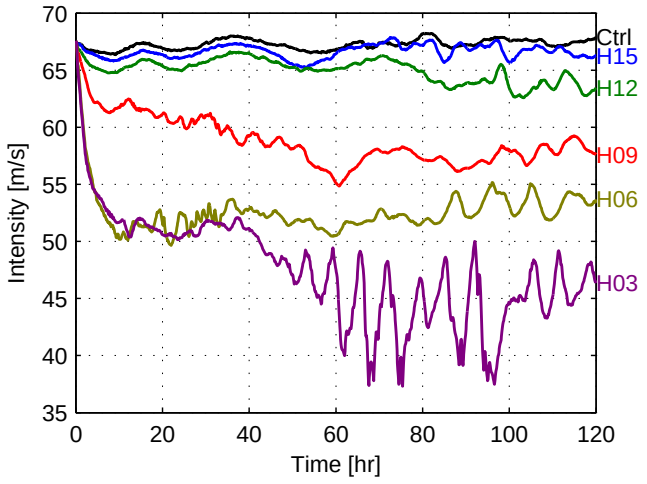

Figure 2: Maximum tangential winds ($\mathrm{m\ s^{-1}}$) in the 'H' ventilation experiments listed in Tab. 1.

In addition the the changes to the TC's structure, the TC intensity decreases with increasing ventilation amplitude, as shown in Fig. 1. For the A01 experiment, the weakening compared to the control run is barely discernible, whereas the TC in the A50 experiment weakens 15 $\mathrm{m\ s^{-1}}$ in the first ten hours. Thereafter, there are two starkly different intensity regimes: a quasi-steady regime and an oscillatory regime. All the experiments are quasi-steady through about 40 hours. The A50 experiment then abruptly transitions to a high frequency oscillatory regime, where the intensity rapidly changes by greater than 10 $\mathrm{m\ s^{-1}}$ in a few hours. Furthermore, the mean intensity during the oscillatory regime is lower than the intensity during the quasi-steady regime.

b. *Height*

In the second set of experiments, the ventilation height is varied from 3 km to 15 km while the amplitude is held at 5.0×10^5 $\mathrm{m^2\ s^{-1}}$. This set of experiments tests the weakening efficacy of ventilation located at various heights in the inner core. The TC intensity time series for these experiments are shown in Fig. 2.

Ventilation is most effective when it occurs at midlevels. The greatest weakening occurs for the H03 experiment, with less weakening occurring as the ventilation layer is moved upward. For upper-level ventilation (H12 and H15 experiments), the TC intensity shows very little difference from the control run. Hence, upper-level ventilation does not appear to be a mechanism that can substantially weaken a TC.

The degree to which ventilation effects the TC is largely determined by whether the eddy mixing can destroy the entropy front at the eyewall. At midlevels, this potential is maximized because there exists a large low-entropy reservoir of relatively dry air in the near-inner core region that the eddies can access. At upper-levels, the radial gradient of entropy is very weak reducing the ventilation potential. Eddy kinetic energy can be very large at upper-levels, but has little to no avail in thermodynamically inducing weakening.

4 Discussion

The change in intensity in the ventilation experiments can be explained using both energy and dynamical diagnostics.

a. *Mechanical Efficiency*

The mechanical efficiency for a steady-state TC is qualitatively given by the following ratio:

$$\epsilon = \frac{\text{Dissipation}}{\text{Surface Fluxes} + \text{Dissipative Heating}}. \qquad (2)$$

For a perfect Carnot engine, this efficiency would be equal to one. This is approximately true in the eyewall of a TC at its potential intensity. However, when considering the mechanical efficiency over the entire TC, the mechanical efficiency is much less than one. The available potential energy generated outside the eyewall by surface fluxes and dissipative heating predominately goes toward moistening and heating the environment. Hence, it is reasonable to expect that ventilation will cause a similar reduction in mechanical efficiency as available potential energy is used to moisten the inner core instead of powering the TC's winds.

The mechanical efficiency for the innermost 100 km and lowest 17 km averaged over 24-48 hours is shown in Fig. 3a for the 'A' ventilation experiments. Interior dissipation and dissipative heating are included because

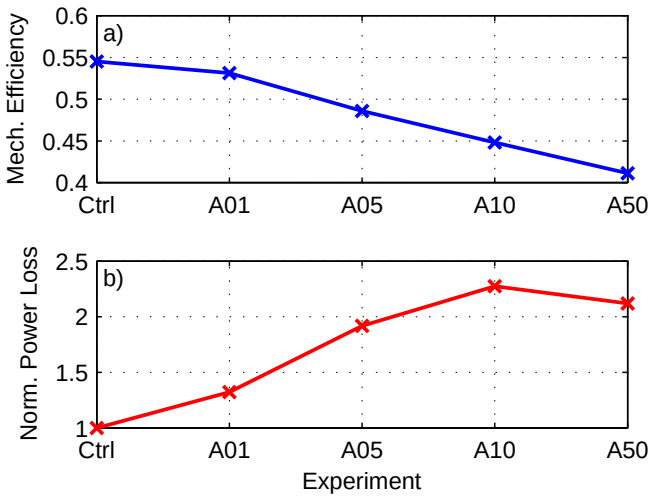

Figure 3: (a) Mechanical efficiency for the 'A' ventilation experiments and (b) the normalized power loss due to turbulent entropy mixing above the boundary layer. Both quantities are calculated for the innermost 100 km and averaged over 24-48 hours.

they are not negligible when integrated over the entire free troposphere. For increasing ventilation amplitude, the mechanical efficiency monotonically decreases from 55% in the control run to 41% in the A50 experiment. Much of the remainder goes into moistening or heating the atmosphere in order to counter the effects of turbulent mixing due to ventilation.

Fig. 3b shows the power lost in the inner core due to turbulent entropy mixing above the boundary layer, which is composed of the direct contribution of the mixing by (1) and the model's turbulence parameterization. Both represent a sink of available potential energy and can be estimated by integrating the product of the divergence of the entropy flux and the difference between the parcels' temperature and reference temperature (Pauluis 2007). The results are normalized by the control run's value. As the ventilation increases, the power loss increases steadily and becomes a larger portion of the total power dissipation[1] in the inner core. In the A05 experiment, the power lost due to turbulent entropy mixing is about twice that of the control experiment. In the A50 experiment, 25% of the total power dissipated is due to turbulent mixing. In contrast, only 9% of the total power dissipated in the control experiment is due to turbulent mixing. Hence, ventilation causes a large percentage of the available potential energy generation from surface fluxes and dissipative heating in the inner core to be destroyed by turbulent mixing above the boundary layer.

[1]The total power dissipated is defined as the sum of frictional and diffusive processes.

b. *Thermal Wind*

Thermal wind balance also provides a simple way of explaining how ventilation affects TC intensity. Presume that the ventilation occurs at a single level. Parcels rising through the eyewall are instantaneously mixed as they cross the ventilation level resulting in an instantaneous reduction in the entropy gradient across the eyewall. Additionally, assume that neutrality holds above and below the ventilation level, such that angular momentum and saturation entropy surfaces are congruent to one another in each separate region. Under such conditions, one can derive a modified thermal wind equation,

$$v_m^2 \approx -M_m \left[c(T_b - T_o) + \Delta c(T_{\mathcal{V}} - T_o)\right] + r_m \zeta_m w_m, \quad (3)$$

where v is the tangential wind speed, M is the angular momentum, T_b is the temperature at the top of the boundary layer, T_o is the outflow temperature, $T_{\mathcal{V}}$ is the temperature at the ventilation level, $c = \partial s^*/\partial M$ is the saturation entropy gradient below the ventilation level, Δc is the jump in the saturation entropy gradient across the ventilation level, ζ is the relative vorticity, and w is the vertical velocity. Any variable with a subscript 'm' is evaluated at the radius of maximum wind (r_m) at the top of the boundary layer. If Δc is zero, then the expression is the classical one from Emanuel (1986), with the last term accounting for unbalanced forces (Bryan and Rotunno 2009).

The theoretical maximum tangential wind speed at the top of the boundary layer in the 'H' ventilation experiments is calculated using (3), where c and Δc are computed using the average saturation entropy gradients across the eyewall above and below the ventilation layer. The theoretical maximum tangential wind along with the actual value at a height of 1 km averaged over 24-48 hours is shown in Fig. 4. The modified thermal wind equation does well at estimating the model's maximum tangential wind speed, particularly when the ventilation is located higher up in the troposphere and the TC is stronger.

The second term in brackets in (3) largely explains the behavior in Fig. 4. The entropy gradient is negative across the eyewall, and ventilation acts to decrease the magnitude of this gradient; thus, Δc is positive. Moving the ventilation to higher levels decreases Δc, since the radial gradient of entropy weakens aloft, and also decreases the value of $T_{\mathcal{V}}$. In the limit that $T_{\mathcal{V}}$=T_o, which is nominally true in the H15 experiment, the ventilation has no bearing on the maximum tangential winds.

c. *Oscillatory Intensity Regime*

The quasi-steady intensity regime is described by the two diagnostics above fairly well since there aren't large time tendencies in the entropy or energy budget. Additionally, the eyewall remains predominately slantwise

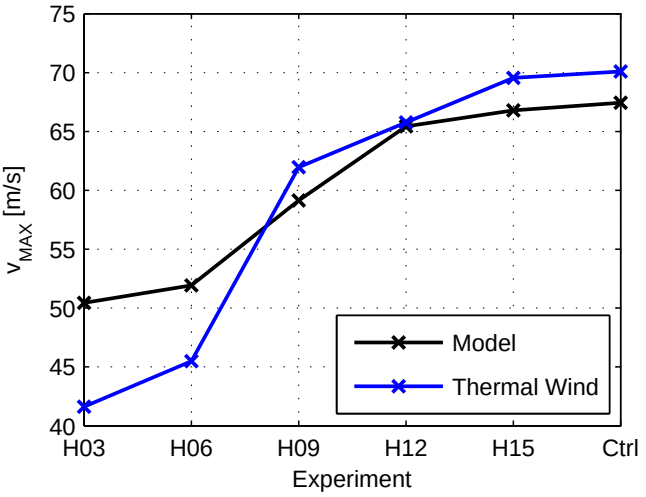

Figure 4: The maximum tangential wind speed (m s^{-1}) at a height of 1 km for the 'H' experiments (black) and the theoretical maximum tangential wind speed using a modified thermal wind equation in the eyewall (blue) averaged over 24-48 hours.

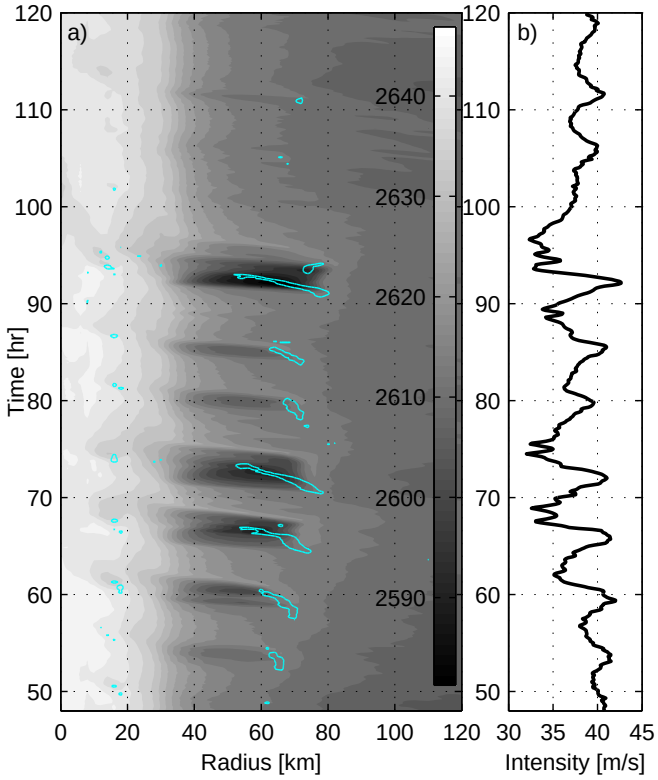

Figure 5: (a) Hovmoller plot of the entropy (J kg^{-1} K^{-1}) at the lowest model level (shading) and downdraft entropy fluxes (m s^{-1} J kg^{-1} K^{-1}) at 1.5 km (cyan outline) and (b) the maximum tangential wind speed (m s^{-1}) at the lowest model level from the A50 experiment.

neutral. This is not true during the oscillatory regime, which is characterized by rapid shifts in the axisymmetric structure of the storm. Each oscillation in the intensity is governed by the life cycle of a convective burst. At first, strong mixing deposits high entropy air into the near-inner core environment resulting in potential slantwise instability. Subsequently, elevated slantwise convection occurs, and precipitation falling from the convective burst evaporates in to the dry air below inducing an intense downdraft of 2-3 m s^{-1}. The downdrafts transport a pocket of low entropy air down into the boundary layer and induce compensating inflow through the middle troposphere resulting in an additional inward flux of low entropy environmental air. The low entropy air in the boundary layer is then swept inwards by the radial inflow stabilizing the atmospheric column and causing convection to temporarily cease until surface fluxes restore the boundary layer entropy. The process then repeats itself with a period of about 5-8 hours.

The life cycle of several of these convective bursts from the A50 experiment is shown in the Hovmoller plot in Fig. 5a. The gray shading is the entropy at the lowest model level (z=150 m), while the cyan outlines denote significant downdraft entropy fluxes at a height of 1.5 km. Each downdraft transports a large amount low entropy into the boundary layer, which is then advected inward. Surface fluxes act to restore the entropy, but not completely before the downdraft modified air reaches the radius of maximum wind around 30 km. The result is a decrease in the radial entropy gradient through a deep layer in the eyewall. In response, the intensity decreases sharply, as seen by the dips in tangential wind speed after each downdraft event in Fig. 5b.

The cumulative effect of the downdrafts also appears to decrease the mean intensity of the storm. Compared to a parallel A50 experiment, in which evaporation is turned off precluding downdraft formation, the A50 experiment is about 5-10 m s^{-1} weaker on average during the oscillatory regime. The downdrafts appear to be occurring frequently enough to significantly affect the entropy budget of the inner core boundary layer and intensity of the storm, as hypothesized by Tang and Emanuel (2010) and Riemer et al. (2010). Only after these large downdraft events cease after 100 hours does the TC begin to recover to a higher mean intensity.

5 Summary

An axisymmetric model is used to assess the sensitivity of a TC to parameterized ventilation. As expected, increasing the amplitude of ventilation weakens the TC by decreasing the mechanical efficiency of the inner core. However, ventilation is most effective at low- to midlevels,

where the entropy difference between the eyewall and environment is the largest, and is less effective as the ventilation increases in height. This is shown to be a consequence of a modified thermal wind equation, in which the entropy gradient jump across the ventilation level becomes weaker and is weighted less at upper-levels. Lastly, the experiments also show quasi-steady and oscillatory intensity regimes. The latter is controlled by transient convective bursts and downdrafts that deposit very low entropy into the boundary layer.

Acknowledgment The authors would like to thank Mike Montgomery and Michael Riemer for their collaboration in this research. This work is supported by NSF grant ATM-0850639.

References

Bryan, G. and R. Rotunno, 2009: Evaluation of an analytical model for the maximum intensity of tropical cyclones. *J. Atmos. Sci.*, **66**, 3042–3060.

Cram, T., J. Persing, M. Montgomery, and S. Braun, 2007: A lagrangian trajectory view on transport and mixing processes between the eye, eyewall, and environment using a high-resolution simulation of Hurricane Bonnie (1998). *J. Atmos. Sci.*, **64**, 1835–1856.

Emanuel, K., 1986: An air-sea interaction theory for tropical cyclones. Part I: Steady-state maintenance. *J. Atmos. Sci.*, **43**, 585–604.

Frank, W. and E. Ritchie, 2001: Effects of vertical wind shear on the intensity and structure of numerically simulated hurricanes. *Mon. Wea. Rev.*, **129**, 2249–2269.

Pauluis, O., 2007: Sources and sinks of available potential energy in a moist atmosphere. *J. Atmos. Sci.*, **64**, 2627–2641.

Riemer, M., M. Montgomery, and M. Nicholls, 2010: A new paradigm for intensity modification of tropical cyclones: Thermodynamic impact of vertical wind shear on the inflow layer. *Atmos. Chem. Phys.*, **10**, 3163–3188.

Rotunno, R. and K. Emanuel, 1987: An airsea interaction theory for tropical cyclones. Part II: Evolutionary study using a nonhydrostatic axisymmetric numerical model. *J. Atmos. Sci.*, **44**, 542–561.

Simpson, R. and R. Riehl, 1958: Mid-tropospheric ventilation as a constraint on hurricane development and maintenance. *Tech. Conf. on Hurricanes*, Amer. Meteor. Soc., Miami Beach, FL, D4–1–D4–10.

Tang, B. and K. Emanuel, 2010: Midlevel ventilation's constraint on tropical cyclone intensity. *J. Atmos. Sci.*, in press.